THE JOURNAL OF COMPARATIVE NEUROLOGY 474:173–189 (2004)

Late Granule Cell Genesis in Quail Cerebellum

ANTONIS STAMATAKIS,[1] HELEN BARBAS,[2] AND CATHERINE R. DERMON[1]*
[1]Department of Biology, University of Crete, Heraklion 714 09, Crete, Greece
[2]Department of Health Sciences, Boston University, Boston, Massachusetts 02215

ABSTRACT

Proliferation of avian cerebellar neurons, including granule cells, is thought to be completed during embryonic life, and aspects of cell addition in cerebellar lobules in posthatching life are unknown. The present study tested the hypothesis that cell genesis in late embryonic and posthatching stages of quail cerebellum occurs in parallel with the performance of motor programs. After exposure to bromodeoxyuridine, short (20 hours) and long survival time points were selected to investigate survival and migration of labeled cells. Quantitative analysis of the lobular distribution of labeled cells was performed with the stereological disector method. External granular layer (EGL) proliferation did not cease after hatching, indicating that there is an extended posthatching period, lasting until P20, when cells can be added into the internal granular layer, modifying the cerebellar circuitry and function. Indeed, long survival experiments suggested that EGL-labeled cells migrated into the internal granular layer and survived for a prolonged time, although many of the progenitor cells remained in the EGL for days. Double-labeling experiments revealed that most of the late-generated granule cells were NeuN positive, but only few expressed nitric oxide synthase. In addition to granule cells, the white matter and a glutamic acid decarboxylase (GAD)-positive cell population in the molecular layer around Purkinje somata showed bromodeoxyuridine labeling. Although all lobules showed significant posthatching proliferation, an anteroposterior gradient was evident. The index of granule cell production and survival supports a spatiotemporal pattern, in correlation with the functional division of cerebellum into anterior and posterior domains. J. Comp. Neurol. 474:173–189, 2004.

Indexing terms: cerebellar development; external granular layer; posthatching proliferation; migration; BrdU immunocytochemistry; stereological disector

The cerebellum, a highly conserved structure, is composed of anteroposterior and mediolateral modular compartments where distinct components of motor behavior are presumably stored and modified when mastering motor tasks or acquiring reflexes (Ito et al., 1982; De Zeeuw et al., 1994; Herrup and Kuemerle, 1997; Ito, 2000). Its laminar pattern and rectilinear geometry (Palay and Chan-Palay, 1974) have long been exploited to provide an important model for understanding the development of normal brain cytoarchitecture and function (Ramon y Cajal, 1911). The progeny of rhombic lip and external granule layer (EGL) progenitors have been determined by retroviral lineage, gene expression, and chick-quail chimeric studies in early stages of avian embryos (Ryder and Cepko, 1994; Lin et al., 2001). Rostral metencephalic and caudal mesencephalic vesicles of embryonic brain participate in the formation of the cerebellum in a topographic order (Hallonet et al., 1990; Hallonet and Le Douarin, 1993; Wassef and Joyner, 1997). Cerebellar cells are produced in two distinct proliferation zones during two distinct time frames: The ventricular zone of the IVth ventricle produces cells early, and the EGL on the surface of the developing cerebellum produces cells later and over an extended period. Cell types known to derive from the

Grant sponsor: the European Union; Grant number: Q5RS-2000-31629; Grant sponsor: Greek General Secretariat Research and Technology (C.R.D.).

In memory of Dr. R. Dermon.

*Correspondence to: Catherine Dermon, Laboratory of Physiology/Neurobiology, Department of Biology, University of Crete, Heraklion 714 09, Crete, Greece. E-mail: dermon@biology.uoc.gr

Received 12 June 2003; Revised 27 October 2003; Accepted 18 December 2003

DOI 10.1002/cne.20066

Published online in Wiley InterScience (www.interscience.wiley.com).

ventricular neuroepithelium include deep cerebellar nuclei neurons, Purkinje cells, interneurons, and glia, as revealed by chick-quail chimeric (Hallonet et al., 1990; Alvarez Otero et al., 1993) and autoradiographic (Hanaway, 1968) studies during early and middle stages of avian cerebellum ontogeny. EGL gives rise to granule cells in birds (Hallonet et al., 1990; Alvarez Otero et al., 1993), as in mammals (Altman, 1972; Rakic, 1973; Gao and Hatten, 1994; Alder et al., 1996; Jankovski et al., 1996; Zhang and Goldman 1996). It is well established that avian EGL originates from a restricted area of the metencephalic alar plate, the rhombic lip, in a topographic manner (Hallonet and Le Douarin, 1993; Marin and Puelles, 1995). The original dorsal, lateral, and ventral portions of the metencephalic alar plate provide cells to the caudomedial, medial, and rostrolateral portions of the EGL. Early and middle phases of avian cerebellum ontogeny are characterized by significant regionalization events underlying patterns of granule cell migration in parasagittal linear arrays (Miale and Sidman, 1961; Feirabend, 1990; Ryder and Cepko, 1994; Marin and Puelles, 1995; Lin and Cepko, 1998; Karam et al., 2001) and gene expression of Eph receptors and ligands (Karam et al., 2000; Blanco et al., 2002). In contrast, cerebellar development patterns during late embryonic and early posthatching stages are not well known for avian species.

The present study provides important, novel quantitative information on the lobular pattern of granule cell production that could be the basis of normal quail cerebellar development, widely used in developmental studies, particularly with chick-quail chimeras as a model (Hallonet et al., 1990; Le Douarin, 1993). We focused on EGL proliferation during the late developmental stages and explored the possibility of an extension of neurogenesis into posthatching life. Different avian developmental patterns exist, and quail, as a precocial bird in terms of development, is capable of moving on its own and behaving independently a few hours after hatching. In contrast, passerine birds (e.g., pigeon) or mammalian species (e.g., rodents) are considered altricial because of their incapacity to move around on their own soon after birth. It is important to note that previous studies in another precocial avian species (chick) have suggested that granule cell genesis is completed in late embryonic life (Hanaway, 1967; Feirabend, 1990).

Previous studies have shown that addition of new cells was related to an avoidance learning paradigm (Dermon et al., 2002) and song learning in birds (Goldman and Nottebohm, 1983; Alvarez-Buylla et al., 1990a; Kirn et al., 1991) as well as sex change in hermaphrodite fish (Zikopoulos et al., 2001). Here we sought to determine whether activity-dependent maturation processes observed in early posthatching life coincide with the addition of new cells in the cerebellar circuits.

MATERIALS AND METHODS

To label cells undergoing cell division, we used the bromodeoxyuridine (BrdU) immunocytochemical method (Miller and Nowakowski, 1988). This method is based on the administration of BrdU, a thymidine analog; its permanent incorporation into DNA of cells during S phase of the cell cycle; and its subsequent immunocytochemical detection. It should be noted that a single injection of BrdU labels the nuclei of cells that are in S phase but not the nuclei of proliferating cells that are in other phases of the cell cycle.

Experimental animals

Experiments were conducted according to the NIH *Guide for the Care and Use of Laboratory Animals* (NIH publication 86-23, revised 1987) and have been approved by the relevant authorities of Crete University. Quail (*Coturnix japonica*) embryos at embryonic days 15 and 16 (E15, E16; n = 10 per stage) and animals at posthatching days 0 (P0; n = 4), 1 (P1; n = 6), 5 (P5; n = 10), 10 (P10; n = 7), 20 (P20; n = 5), and 50 (P50; n = 3) were used for the determination of proliferation patterns in the developing cerebellum. All animals were obtained from our own colony by incubation of fertilized eggs (purchased from a local dealer) in a humidified incubator at 38.3°C. Animals hatched after 17 days of incubation. The first 24 hours after hatching were assigned as posthatching day 0 (P0). Hatchlings were kept on an 18L:6D light cycle at 30°C and had access to food and water ad libidum, except for a period of 3 hours following BrdU administration, when food was withheld to maximize BrdU incorporation into DNA.

BrdU administration

To label cells in the S phase of posthatching quail, a pulse of intraperitoneal injection of BrdU (100 mg/kg body weight in 200 μl sterile saline) was administered at P0, P1, P5, P10, P20, and P50, and animals were allowed to survive for 20 hours (short survival). To study the migration and survival of the newborn cells, animals were allowed to survive until P20 (long survival). At selected stages, animals were allowed to survive until P50. Preliminary experiments were also performed with 3- and 6-hour survival times to ensure the site of cell birth and the maximal labeling of newborn cells.

For the two embryonic stages studied (E15, E16), eggs were windowed, and BrdU solution (0.1 mg/g) was applied on top of the air sac blood vessels, a site that permits rapid entrance into the blood stream. This is supported by the fact that, 3 hours post-BrdU application, labeled cells were found in the EGL. This type of BrdU application differs significantly in terms of BrdU availability from previous methods used for avian eggs, in which injections were made into the yolk sac, where ^{3}H-thymidine remains available for 48 hours (Yurkewicz et al., 1981). Our method could be considered a modification of direct application into the circulatory system (Striedter and Keefer, 2000), as pulse labeling of proliferating cells with no more than 24 hours of duration.

Early/intermediate embryonic neuroblasts of chick mesencephalon and spinal cord have a cell cycle of 15–16 hours, with S phase lasting 5–6 hours (Fujita, 1962; Wilson, 1973), whereas early postnatal mammalian EGL cells have a longer cell cycle lasting for 16–19 hours and S phase 9–11 hours (Schultze and Korr, 1981). We assumed, based on evidence that cell cycle duration increases with progression in embryonic age and that most of the increase is due to an increase in G1 phase, whereas S phase seems fairly constant (Caviness et al., 1995; Nowakowski et al., 2002), a cell cycle duration of at least 20 hours for the developmental stages examined. Therefore, in the short-term survival time (20 hours), the BrdU injected was likely available for only one cell cycle until the animal was killed, although it is unclear whether BrdU was avail-

able for the entire 20-hour survival period or in only a limited time window. In mammals, BrdU incorporation into DNA continues for approximately 5–6 hours after administration (Hayes and Nowakowski, 2000), and in fish for only 2–4 hours (Zupanc and Horschke, 1995), but no data are available for avian species. In case BrdU was available for a shorter time, $BrdU^+$ cells would be a fraction of the total number of cells born during the entire survival period. This would lead to underestimation of cell numbers, although the developmental comparisons would not necessarily be affected if the BrdU bioavailability was similar during the developmental periods compared. For the long-term survival groups, however, proliferating cells labeled at 20 hours will produce labeled daughter cells if they continue to divide, as shown in mammals (Hayes and Nowakowski, 2002). In this case, the number of cells detected as labeled at the longer survival times would be greater than the number detected as labeled at the shorter survival times.

We note that BrdU may have an adverse effect on embryonic development, including embryonic malformations, such as cleft palate, and neural tube defects, and may interfere with the normal cell cycle and naturally occurring cell death (Yu, 1977; Bannigan and Langman, 1979). However, BrdU doses used in those studies were five to nine times higher than those used here. Moreover, the injections were made in early embryonic stages in previous studies, instead of in the late embryonic stages and hatchlings used here. We observed no morphological or apparent motor or behavioral malfunction in our quail hatchlings injected with BrdU.

BrdU immunocytochemistry

Animals were deeply anesthetized with chloroform and transcardially perfused with ice-cold fixative solution [4% paraformaldehyde in 0.01 M phosphate-buffered saline (PBS), pH 7.4, 25°C]. The brains were removed from the skull, and the cerebellum was dissected and postfixed at 4°C overnight in the same fixative, frozen in isopentane at −40°C, and stored at −80°C until immunocytochemistry was performed.

The cerebellum was cut on a cryostat (Leica CM 1500) into transverse and sagittal sections at 50 μm. One section every 150 μm was kept in phosphate buffer (PB; 0.1 M, pH 7.4). To denature DNA, sections were treated with 2 N HCl for 30 minutes at room temperature; thoroughly washed (6 × 5 minutes) in 0.01 M PBS, pH 7.4; immersed in blocking solution (1.5% normal horse serum, 0.2% Triton X-100 in PBS); and incubated overnight at 8°C with a mouse anti-BrdU monoclonal antibody (Becton Dickinson, San Jose, CA; diluted 1:100 in 0.01 M PBS). Sections were then rinsed in PBS (3 × 5 minutes); incubated in biotinylated anti-mouse IgG antibody (Vector, Burlingame, CA; diluted 1:200 in 0.01 M PBS) for 2 hours at room temperature; rinsed in a solution containing 0.2% Triton X-100 in 0.01 M PBS, pH 7.4; and incubated in an avidin-biotin-peroxidase solution (Vector ABC Elite kit, diluted 1/50 A and 1/50 B in 0.2% Triton X-100 in 0.01 M PBS, pH 7.4) for 1 hour in the dark at room temperature. The incubation was followed by consecutive rinsing in 0.01 M PBS, pH 7.4, and 25 mM Tris-buffered saline (TBS), pH 7.5. $BrdU^+$ cells were visualized by the brown precipitate of peroxidase-catalyzed polymerization of 1.5 mg/ml diaminobenzidine (DAB) in the presence of 0.01% H_2O_2 in TBS. Reaction was terminated by repeated washes in ice-cold TBS, pH 7.5. Sections were mounted on chrome alum/gelatin-coated slides, dehydrated, and coverslipped with Entellan (Merck, Darmstadt, Germany).

To detect nonspecific labeling, adjacent sections were incubated in the absence of the primary or the secondary antibody or the ABC solution, and in each case there was no detectable labeling. Additional control animals with no BrdU injection were prepared, perfused, and BrdU immunoassayed with primary and secondary antibodies, as previously described, to exclude the possibility of false-positive labeling. No labeling was present in these control experiments. For identification of cytoarchitectonic boundaries and the type of BrdU-labeled cells, sections were counterstained with either methyl green (1% in ddH_2O) or cresyl violet (0.5% in ddH_2O).

Quantitative analysis

BrdU-labeled cells were viewed under a microscope using brightfield illumination (Nikon Optiphot-2). Each cerebellar lobule was analyzed separately. For each brain in the short-term survival group, we determined the presence of labeled cells in cerebellar layers. For all animals studied, every other section was analyzed (9–12 sections) and the average percentage of $BrdU^+$ cells within each layer of each lobule was calculated. The identification of laminar boarders was based on the Nissl staining. For the EGL, we employed the stereological disector method (Sterio, 1984; Gundersen et al., 1988) to estimate the number of cells labeled at each developmental stage studied. We used a modification of the physical disector; instead of using two adjacent sections as reference and lookup, the two sides of one section, i.e., front vs. back, served as such. The more widely used optical disector could not be applied here, because labeling did not completely penetrate the sections. In a pilot study, we determined the optimal size of the counting frame (1,150 μm^2) as well as the sampling distance. Sampling distance depended on the size of the cerebellum, which, in turn, depended on the developmental stage of the animal. We estimated lobule volumes according to the Cavalieri (1966) method. The same stereological analysis was performed for EGL and internal granular layer (IGL) of animals in the long-term survival groups. All immunoreactive cells were considered $BrdU^+$, regardless the intensity of labeling.

Double-labeling experiments

To investigate the type of $BrdU^+$ cells, we performed double-labeling experiments in selected developmental stages of the long survival groups. To test whether BrdU-labeled cells were neurons or glia, we used double immunolabeling for BrdU and NeuN, a useful neuronal marker for most neuronal types (Mullen et al., 1992). To define more specifically the phenotype of the BrdU-labeled cells, we performed double immunolabeling for BrdU and glutamic acid decarboxylase (GAD), characterizing neurons synthesizing γ-aminobutyric acid (GABA; Spiro et al., 1999; Benagiano et al., 2000). NeuN or GAD immunolabeling was followed by BrdU immunocytochemistry, with the following modifications. Sections were immersed in blocking solution for 1 hour, incubated for 24 hours at 8°C with the monoclonal anti-NeuN (Chemicon, Temecula, CA; 1:500 in 0.01 M PBS with 0.1% Triton X) or rabbit polyclonal anti-GAD (Sigma, St. Louis, MO; α-GAD 1:1,000 in PBS with 1% Triton X and 0.15% HNS), and rinsed (2 × 5 minutes) in 0.01 M PBS. For NeuN and GAD

detection, sections were incubated with secondary fluorescent antibody for 2 hours (α-mouse Alexa Fluor 568, 1:200 in PBS, and anti-rabbit antibody; Jackson Immunoresearch, West Grove, PA; Cy3, 1:1,000 in PBS with 1% Triton X, both labeling cells red, respectively). After NeuN and GAD immunolabeling, BrdU immunocytochemistry was performed as described previously, by using a fluorescent primary antibody [Beckton-Dickinson, San Jose, CA; α-BrdU, fluorescein isothiocyanate (FITC), 1:100 in PBS, overnight, 8°C, labeling cells green]. Sections were observed under a fluorescence microscope (Nikon Eclipse 800).

To investigate whether some newborn cells were neurons containing nitric oxide synthase (NOS), we performed NADPH-diaphorase histochemistry prior to BrdU immunolabeling, according to a modified method (Dermon and Stamatakis, 1994; Dombrowski and Barbas, 1996). Cerebellum was processed and cut as for single BrdU immunocytochemistry. Free-floating sections were washed (3 × 10 minutes, 37°C) in 0.1 M Tris HCl (pH 7.4, 25°C) and then reacted with 0.8 mM NADPH (Sigma), 0.9 mM nitroblue tetrazolium (Sigma), 10 mM malic acid (Sigma), and a drop of Triton X, with gentle agitation for 15–20 minutes at 45°C in the dark. The reaction was terminated by repeated rinsing with ice-cold 0.1 M Tris HCl. After NADPH-diaphorase, BrdU immunocytochemistry was performed as described for single BrdU-labeling experiments.

Photomicrograph production

High-resolution microscopic images were digitally captured using a color 3CCD Sony DXC-950P camera on a Nikon Eclipse E800 microscope connected to a PC via a Scion CG-7 frame grabber (Scion Corp.). Composite photomicrographs were prepared with the Adobe Photoshop 6.0 (Adobe Systems, Mountain View, CA). The schematic drawing in Figure 2 was prepared electronically: A digitally captured image of cerebellum was transferred to CorelDraw 11, and the outline of lobules was drawn.

RESULTS

The cerebellar volume increased during the developmental period studied from 20 mm^3 at E15 to 80 mm^3 at P50, with significant growth occurring between P10 and P50 days (Fig. 1A). The volume change of each lobule in the developmental stages studied is shown in Figure 1B,C for the anterior and posterior cerebellum, respectively. However, the volume percentage of each lobule with respect to the total cerebellar volume remained constant throughout the developmental stages (Fig. 2), suggesting a preserved relationship among lobules. Lobules I and X represented the smallest (2% and 4%, respectively) and lobules VII, VIII, and IX the highest (11%, 13%, and 11%, respectively) proportion of the cerebellum, whereas deep nuclei and white matter occupied about 19% of total cerebellum volume (Fig. 2). Cerebellar volume growth is due mainly to the addition of new parallel fibers (Rakic, 1973), which, in turn, depends on the addition of new granule cells produced in the EGL. Not surprisingly, the number of newborn cells in the EGL of cerebellar lobules at each stage correlated well with the volume of the lobule (Pearson R = 0.85–0.7, $P < .01$).

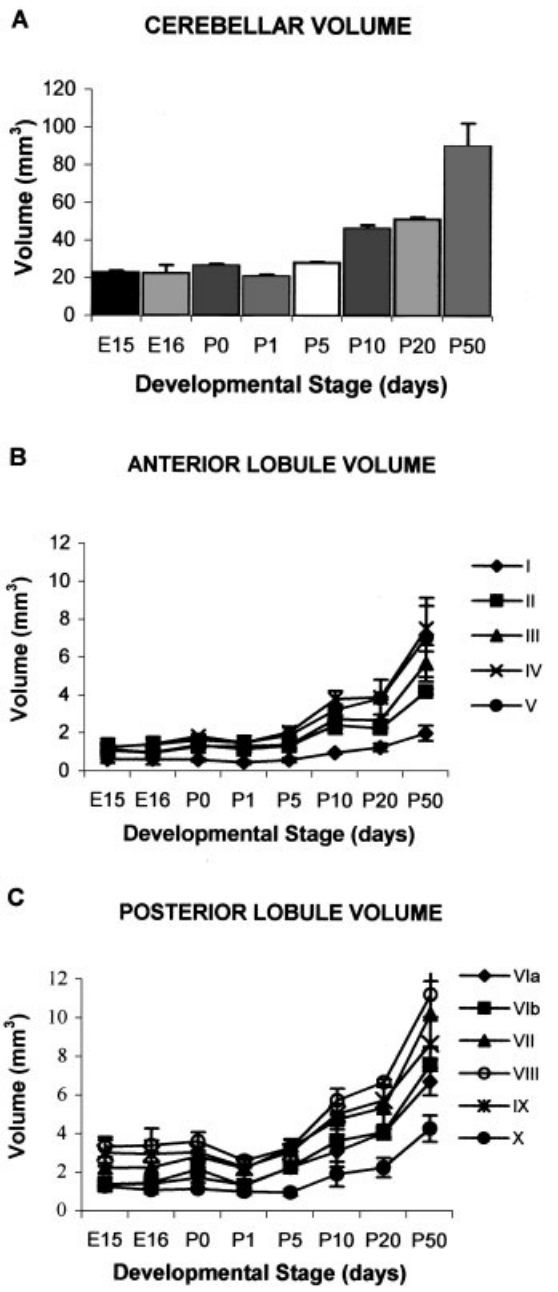

Fig. 1. **A:** Quail total cerebellar volume (mm^3) at late embryonic (E15, E16) and posthatching (P1, P5, P10, P20, P50) ages. Significant changes in the volume occur between P5–P10 and P20–P50. Diagrammatic presentation of regional volume changes with age is shown in **B** for anterior lobules and in **C** for posterior lobules.

Short-term survival: labeled cells 20 hours post-BrdU application

Twenty hours post-BrdU application, the vast majority of $BrdU^+$ cells in the quail cerebellum was found in the EGL, but some were also noted in the molecular layer and the IGL as well as the white matter, at all ages studied (E15, E16, P0, P1, P5, P10, P20, P50). It is noteworthy that proliferation persisted at significant levels at post-

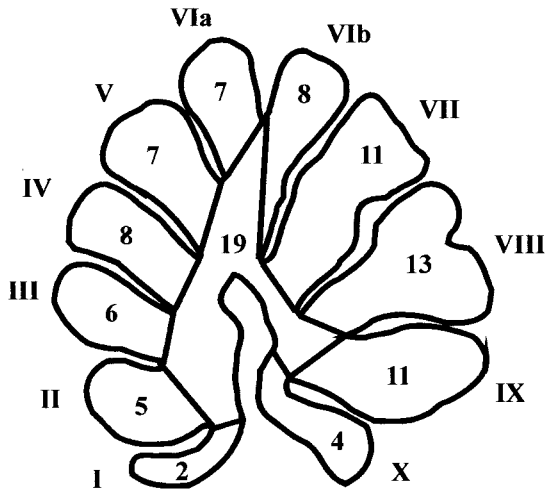

Fig. 2. Schematic presentation of parasagittal cerebellar view. Each lobule represents a volume percentage of the whole cerebellum. The volume percentage of each lobule is indicated as a number within the lobule and does not change as cerebellar size increases.

hatching days, and a few labeled cells were found in the EGL even at P20 and P50.

EGL. The EGL was present as a germinal zone covering the cerebellar lobules at all stages studied. Microscopic observation of Nissl-stained sections showed that its width gradually reduced with age from about seven to ten cell rows at E15 to one or two cell rows at P20. At E15 and E16, high densities of $BrdU^+$ cells were observed in the EGL (Fig. 3A,B), whereas, at P20 and P50, relatively fewer cells could be found (Fig. 3G,H). At P5 and P10, the labeled cells covered most but not all of the EGL surface, and, at P20 and P50, individual $BrdU^+$ cells were found scattered in a superficial position. All cerebellar lobules showed steadily declining $BrdU^+$ labeling from late embryonic ages until P20 (Fig. 3). With the volume of each lobule at each developmental stage taken into account, the proliferative activity was expressed as density (number of cells/mm^3) of labeled cells (Fig. 4A). At most developmental stages, lobule I exhibited the highest density of labeled cells, amounting to approximately double that of all other lobules. At E15, the highest density of $BrdU^+$ cells was found in lobules I, VII, VIb, and II, whereas, at E16, lobule II exhibited the highest density of labeled cells, followed by lobules VII, VIb, V, and I. At posthatching stages, the density of newborn cells was similar in most lobules except for lobule I, ranging from 3,220 to 6,098 cells/mm^3 at PO, 2,577–5,393 cells/mm^3 at P1, and gradually declining to 552–1,878 cells/mm^3 at P20 (Fig. 4A).

The total number of labeled cells within each lobule is presented in Figure 4B. Lobule VIII, the largest lobule in the cerebellum, included the highest number of labeled cells at almost all stages studied. The time course of generation of new cells within individual lobules varied, so that lobules I, II, VII, VIII, and IX included maximal numbers of labeled cells at E15–E16. Lobules V, VIb, VII, VIII, and IX showed the highest proliferation rates for the first days of life after hatching (P0–P1). Figure 5A illustrates in a stack bar graph format the total number of $BrdU^+$ cells determined for each lobule at a specific developmental stage, for the whole period studied. This nicely illustrates the contribution (cell addition) of a specific stage for each lobule and emphasizes the differences in the course of maturation of the different lobules. Lobules that formed early were distinguished from late-forming lobules by a relatively low proportion of labeled cells in posthatching ages and an earlier decline in the width of the EGL. For example, in lobules I, VII, and IX at E15 and E16, cell proliferation represented 49–52% of the total labeled cells for all stages studied, indicating their early formation (Fig. 5B). In contrast, lobules III and IV have a prolonged maturation; i.e., the production of granule cells proceeded in a rather constant manner until day P20 (representing at each stage 14–18% of the total labeled cells). A common characteristic of the developmental profile of most lobules was a transient increase of neurogenesis at P10. At a later stage (P20), lobules III and IV included significant proportions of labeled cells, which is important.

Molecular layer. Twenty hours post-BrdU, the molecular layer of all cerebellar lobules included only a few labeled cells during the developmental periods studied (Fig. 3). Their number gradually declined until day P50, when very few labeled cells could be detected. Some of these cells had the appearance of migrating granular neurons, with elongated cell somata, based on observation of Nissl-stained sections (Fig. 3A, E15 lobule I, arrow); this finding is consistent with the idea that they were cells generated in the EGL within the previous 20 hours. Sections treated to detect NADPH-diaphorase differentiated the molecular layer into an outer sublayer exhibiting lower diaphorase activity and an inner sublayer close to the granular layer, noted from E16 throughout all developmental stages studied (data not shown). The significance of this low expression of NOS, possibly by the later-forming parallel fibers (Rakic, 1973), remains to be explored but could be related to the lack of NOS activity of the later-generated population of granule cells. At these early posthatch stages, confocal microscopy revealed expansion of dendritic arborization of avian Purkinje cells (Mori and Matsushima 2002). This NADPH-diaphorase pattern did not relate to the $BrdU^+$ cells, which were evenly distributed throughout both molecular sublayers.

IGL. As early as 20 hours post-BrdU injection, large numbers of labeled cells were noted within the IGL, at all stages studied, but these decreased gradually with age. Labeled cells found in the IGL within 20 hours from BrdU application could represent granule cells that were produced in EGL and completed their migration, or proliferating population, glial cell progenitors. Specifically, the labeled granule cells following BrdU injection at E15 resulted in high numbers of labeled cells in the granular layer (Fig. 3A,B); labeled cells were topographically organized and were distributed mainly in the superficial part of the IGL, close to the Purkinje cell layer (Fig. 3A,B). The likelihood that the labeled cells in this location represent a proliferating population that may produce Bergman glial cells is addressed in the genesis of other cell populations in the Discussion.

NADPH-diaphorase activity within the granular layer was lower in lobules I and II compared with the rest and gradually decreased in all lobules with age. At P50, we observed two interlayer intensities, in lobules I–V and VIb, dividing the granular layer into superficial and deep zones, where the sublayer close to the Purkinje cell layer exhibited darker staining.

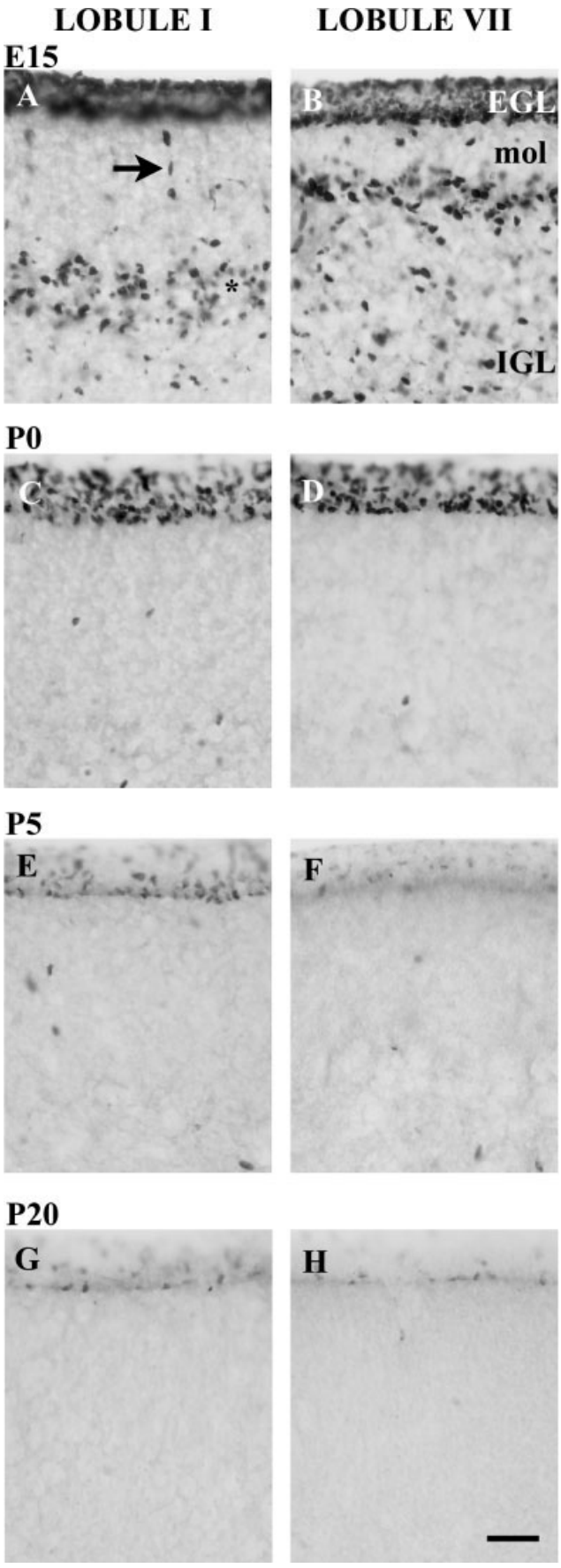

White matter. In the cerebellar white matter, levels of $BrdU^+$ cells were remarkably different between early and late posthatching stages (Fig. 6). Whereas, at E15, E16, and P0, moderate numbers of $BrdU^+$ cells were present in the white matter of all cerebellar lobules, the number gradually decreased posthatching until P20, when almost no labeled cells could be detected in the white matter of any lobule. An exception was seen for lobules VIa, VIb, where a few labeled cells were present at P10 and P20. Lobules I and X included only a thin layer of white matter, which could not be easily distinguished from the granular layer.

Long-term survival: labeled cells at specific stages determined at P20 and P50

To investigate the fate of the EGL cells, animals were injected with BrdU at days E15, E16, P1, P5, and P10 and allowed to survive until day P20. In addition, a few animals were allowed to survive until P50. The major focus of investigation centered on cells born in EGL that migrated to the IGL (Fig. 7), because these were the most numerous, although some cells were found in other layers of specific lobules. Labeled cells within the IGL showed different degrees in labeling (intensely to lightly labeled; Fig. 7). Density measurements of labeled cells within the IGL (number of $BrdU^+$ cells vs. total number of granule cells) were performed in five adjacent counterstained sections of each animal to obtain an estimate of the contribution of late-generated cells to the IGL at P20. Approximately 12% and 8% of the IGL cells were labeled at E16 and posthatching stages, respectively. These percentages represent a rough indication of survival, proliferation, and cell death events, insofar as no stereological analysis was performed, and the cell cycle parameters and number of further divisions or apoptosis of the labeled cells are not known.

However, not all labeled cells migrated away from their place of origin in the EGL. A few cells labeled at the stages studied were still found in the EGL at P20 day. Specifically, labeled cells at embryonic stages E15 and E16 remained in EGL of lobules II, III, and VIb until at least P20. In addition, a few cells labeled at early posthatching stages were still present in the EGL at day P20 (labeled at P1 in lobule V; labeled at P5 in lobules I and VIa–VIII, X; labeled at P10 in lobules III, IV, VII, and VIII). However, by day P50, all labeled cell had moved away from the EGL.

Long-term intervals: BrdU labeling at E15 and E16. Most of the cells of the EGL that were labeled at embryonic stages E15 and E16 had migrated to the granular layer by day P20 (Fig. 8A,B), but their distribution pattern within IGL was still clearly heterogeneous, similarly to their localization in short survival experiments. That is, we observed in most lobules an outside-inside gradient of labeled cells in IGL, with the outer part of IGL (i.e., closer

Fig. 3. External granular layer mitotic activity at different developmental stages of quail cerebellum 20 hours post-BrdU application. Photomicrographs of parasagittal sections showing the distribution of $BrdU^+$ cells within cerebellar layers of representative lobules of archi (lobule I; **A,C,E,G**)- and neo (lobule VII; **B,D,F,H**)-cerebellum at days E15 (A,B), P0 (C,D), P5 (E,F), and P20 (G,H). Arrow in A points to migrating cells in a line. EGL, external granular layer; IGL, internal granular layer; mol, molecular layer. Scale bar = 20 μm.

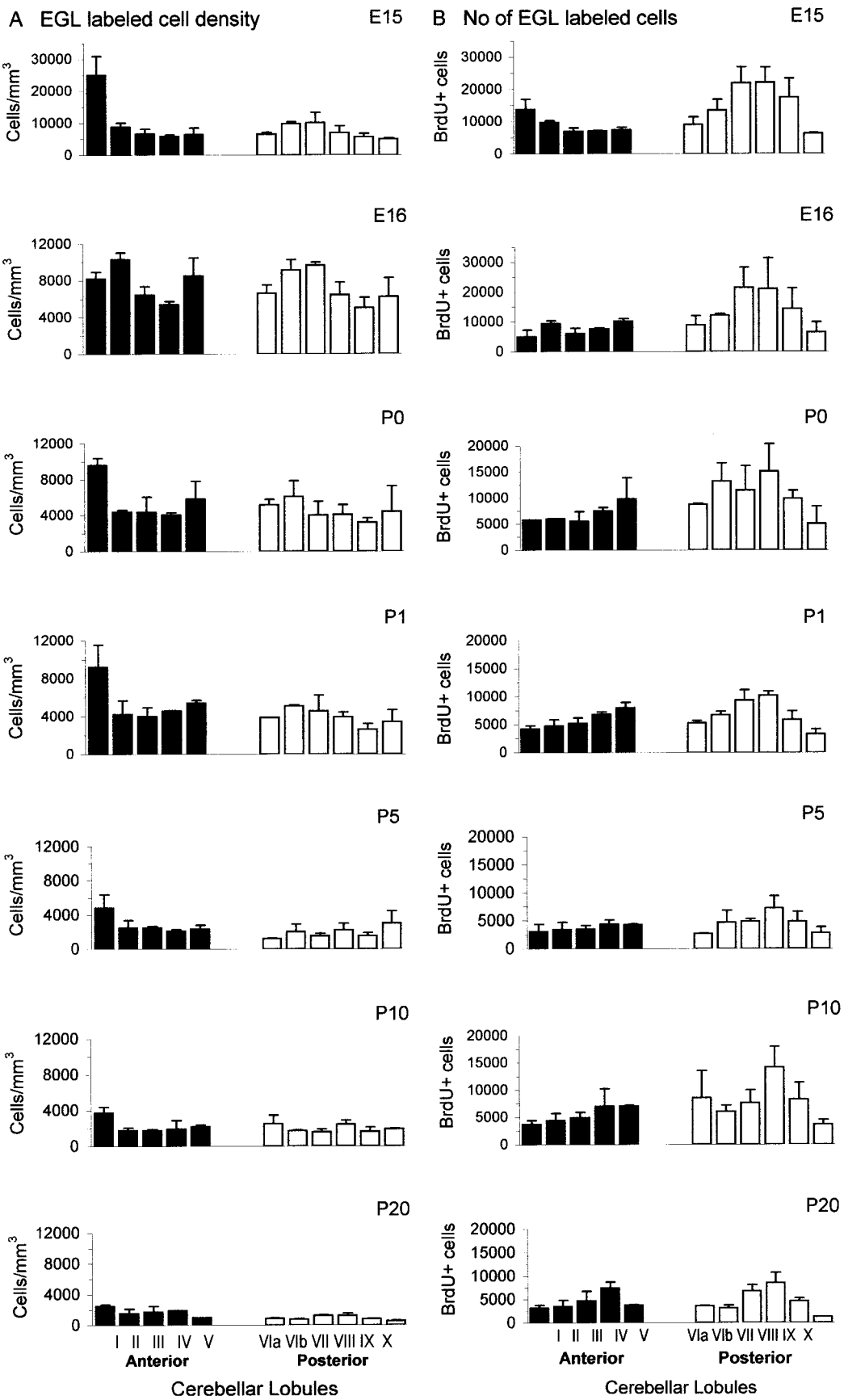

Fig. 4. EGL proliferation in individual lobules at E15–E16 and at P0–P20. Labeled cells determined 20 hours post-BrdU application were estimated by using the disector method. Solid and open bars differentiate lobules of the anterior and posterior cerebellar lobe, respectively. **A:** Density of $BrdU^+$ cells (cell/mm^3) within EGL of individual lobules. **B:** Total number of $BrdU^+$ cells within EGL of individual lobules. Note that the ordinate varies among graphs, for optimal visualization of changes.

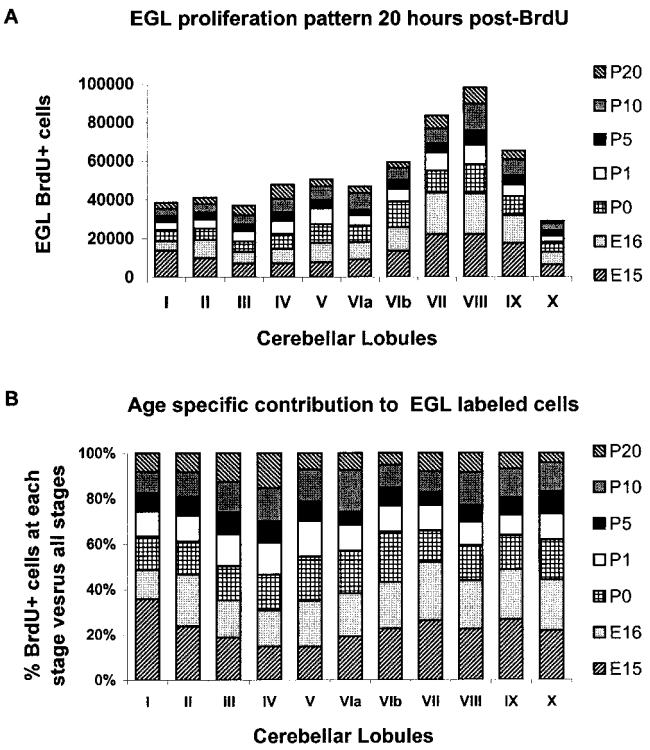

Fig. 5. **A:** Age-specific EGL proliferation 20 hours post-BrdU application. The contribution of specific developmental stages to the total of EGL cell proliferationis shown as stacks in the bars, with earlier stages at the bottom of the bars. **B:** Lobular pattern of the percentage of $BrdU^+$ cells determined at a specific stage vs. the total $BrdU^+$ cells at all stages studied. Embryonic proliferation (E15, E16) accounted for about 50% of the cell production in lobules I, VII, and IX, whereas, for the other lobules, most cells determined from E15 to P20 were born after hatching. The patterns indicating the ages are shown at right.

to the Purkinje cell layer) showing a higher density of $BrdU^+$ cells (Fig. 9). In addition, in lobule VIa and mainly lobule VII, a clear rostrocaudal pattern was noted in the final position of the labeled cells at E15. Specifically, in the rostral compartment of lobules VIa and VII, the IGL was nearly devoid of $BrdU^+$ cells, whereas the caudal part included a high density of positive cells (Fig. 9B). This rostrocaudal gradient in the final position of labeled granule cells did not characterize short-term experiments that determined their progenitor cells (that is, the distribution of labeled EGL cells 20 hours post-BrdU, in VIa and VII or any other lobule). This lack of labeled granule cells in the IGL of the anterior pole of the above-mentioned lobules after long-term survival is interesting, particularly in that the overlying EGL of the rostral pole was densely labeled 20 hours post-BrdU (Fig. 9A). Therefore, the progenitor cells labeled while in the EGL (their proliferation site) were no longer present in the EGL (no significant labeling was found in the EGL at P20) but had not move radially to the underlying IGL of the rostral part of lobules VII and VIa (Fig. 9B). These cells labeled at E15 did not contribute to the population of granule cells of rostral lobules VII and VIa, suggesting either their tangential migration in a different parasagittal domain or their apoptosis. Such nonribboned migration with no respect to the PC compartmentalization is suggested to occur late in development (Komuro and Rakic, 1998). This speculation on possible tangential migration or apoptosis is based on the assumption that the specific part of the EGL of these lobules at this stage is producing postmitotic cells. However, it is possible that the specific parts of EGL are not yet producing any postmitotic cells and that labeling is diluted and no longer detectable because of continued proliferation, presumably with only symmetric nonterminal divisions (Hayes and Nowakowski, 2002). This observation supports the idea that the onset of granule cell production differs among lobules.

In addition to the granule cells, round cells labeled at E15 and E16 were localized in the molecular layer bordering the Purkinje cell layer and within the Purkinje cell layer surrounding Purkinje cell somata (PC) by P20 (Fig. 8A,B). These labeled cells could be classified into two groups based on their size: 2–3μm in diameter (small cell type; arrowheads in Fig. 8) and 7–10 μm in diameter (medium-sized cell type; arrows in Fig. 8), evenly distributed within and around the PC layer. It is important to note that this labeled cell population did not exhibit any rostrocaudal gradient, as was found for a subpopulation of granule cells in long-term survival. A few labeled cells were also present in the molecular layer of most lobules (Fig. 8B), except for lobule VIII, as well as in the white matter of lobules II–VIa and VII. Double-labeling experiments with GAD, NeuN, and BrdU immunocytochemistry revealed that most of the $BrdU^+$ cells were $NeuN^+$ and that those located next to PC in the molecular layer expressed GAD (Fig. 9G–I).

Long term intervals: post-BrdU labeling at P1, P5, and P10. By day P20, the majority of cells born in EGL at day P1 had migrated into the IGL (Fig. 7A), although a few $BrdU^+$ cells were also detected in the molecular layer (mainly in lobules II and III; Fig. 8C), but none was seen in the white matter. In double-labeling experiments, some of the $BrdU^+$ cells showed NADPH-diaphorase activity (Fig. 9C), suggesting that they are granule cells expressing NOS. Similarly, cells born in the EGL at P5 and P10 had migrated to IGL by day P20 (Fig. 7B,C). In addition, some labeled cells were found in the molecular layer of lobules I–IV, VIb, and VIII–IX as well as in the white matter of lobules III–V. EGL cells proliferated also at day P20 and migrated into the IGL by day P50. Double-labeling experiments with NeuN and BrdU immunocytochemistry revealed that most of the $BrdU^+$ cells were $NeuN^+$ (Fig. 9D–F). No outside-inside gradient of the final position of BrdU-labeled cells in the IGL was found for the posthatching generated granule cells.

Figure 10A shows the specific addition of labeled granule cells in the IGL of cerebellar lobules at P20, after long survival periods. The regional differences in granule cell production and survival in the stages investigated suggest that lobules VIb, VIII, and X included a higher proportion of granule cells labeled at embryonic day 16, whereas, in lobules II, III, IV, V, VIa, VII, and IX, most late-generated granule cells were labeled after hatching (Fig. 10B).

Ratio of labeled cells in long/short intervals (index of survival vs. proliferation)

To investigate the survival of the EGL labeled cell population (future granule cells), we compared the number of

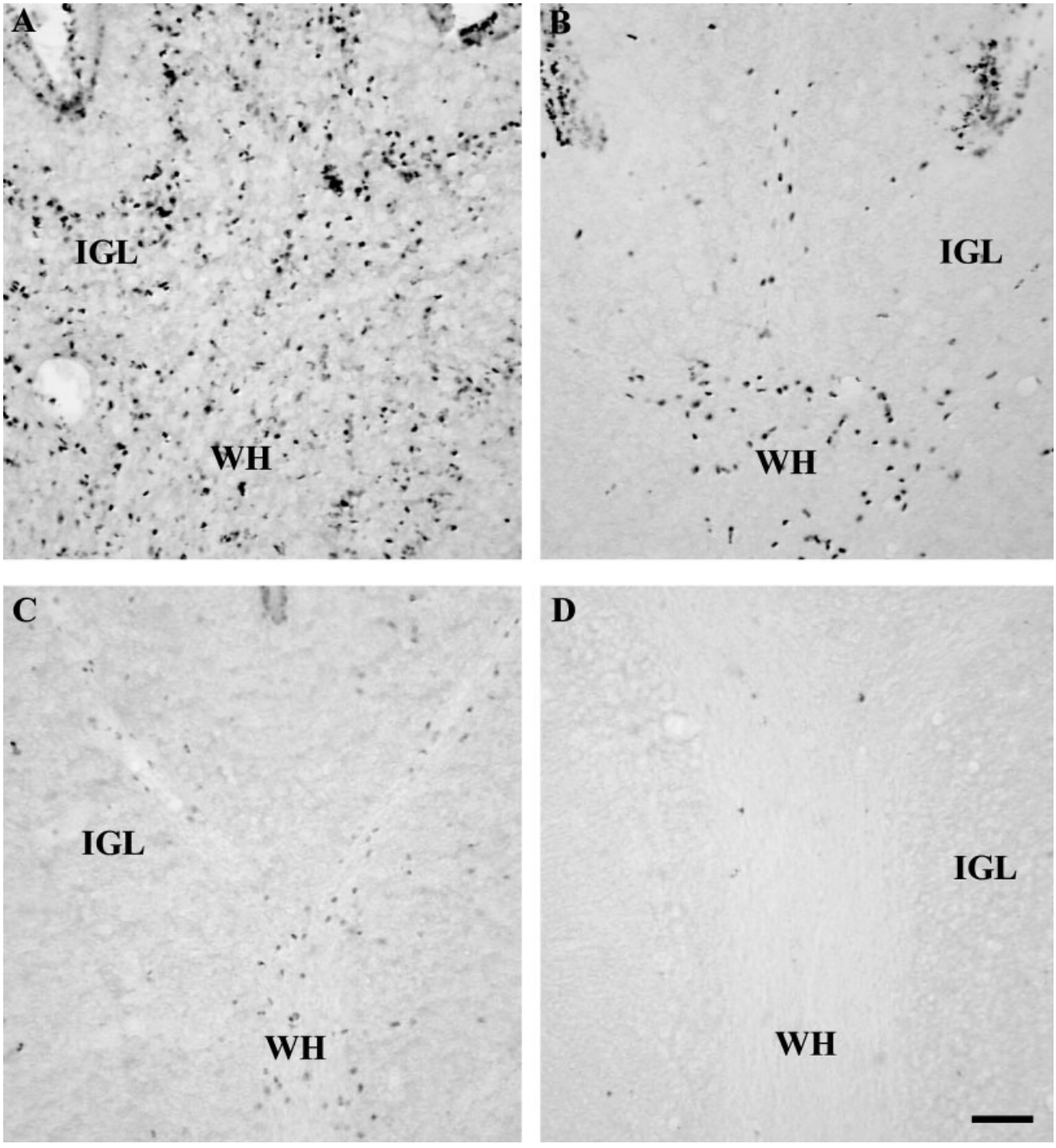

Fig. 6. Labeled cells found within the cerebellar white matter 20 hours post-BrdU injection. Photomicrographs of parasagittal cerebellar sections showing the distribution of labeled cells in the white matter following BrdU application at E15 (**A**), P1 (**B**), P5 (**C**), and P20 (**D**). In most cases, cells encountered were elongated, indicating migratory activity. IGL, internal granular layer; WH, white matter. Scale bar = 50 μm.

$BrdU^+$ cells, labeled at a specific developmental age, at two survival points (short-term, 20 hours; long-term, P20). This comparison produced a labeling index of survival vs. proliferation, determined by the ratio of labeled cells at long and short intervals. For the 20-hour survival time, we chose to ignore the few $BrdU^+$ cells that were not in the EGL, because their number was very low compared with the number of $BrdU^+$ cells present in the EGL, essentially not affecting the data. Note that, in posthatching experiments, 20 hours is less than the cell cycle length (plus the

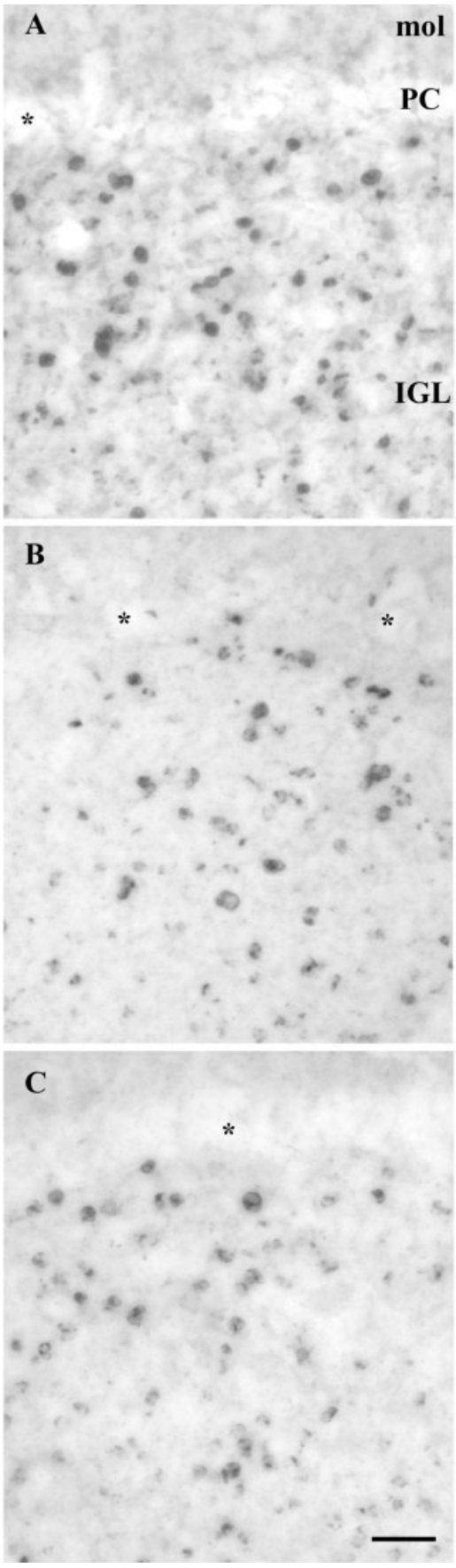

waiting time in the deep EGL), as evidenced by our data and from previous studies in mammals based on ^{3}H-thymidine autoradiography (Fujita et al., 1966; Rakic, 1971, 1973), cell cycle length (Caviness et al., 1995; Nowakowski et al., 2002), and real-time observation of the prospective granule cells after their last mitosis in living slice preparations (Komuro et al., 2001). When labeled cells in the EGL exited the cell cycle, they migrated to the IGL, where they were encountered at P20. However, some of these EGL cells, before migrating, reentered the cell cycle and produced daughter cells for the next three or four cycles (Hayes and Nowakowski, 2002). With this evidence taken into account, the number determined by the ratio of labeled cells in long survival vs. short survival could be referred to as the survival index. This survival index does not represent an absolute reference, in that cell cycle parameters differ among lobules and developmental stage, but it does represent an integration of proliferative and cell death events occurring during long-term survival. Most lobules showed two- to fourfold increases in the number of positive cells residing in the IGL by day P20 compared with those labeled in the EGL 20 hours post-BrdU (Fig. 11). Specifically, major increases were noted for cells born at E16 in lobules III–VIb and VIII (Fig. 11A); at P1 in lobules IV, VIa, and VIB (Fig. 11B); at P5 in lobules VIa and VII–IX (Fig. 11C); and at P10 in lobules III, VII, and X (Fig. 11D). However, in some lobules, the numbers of BrdU^{+} cells in the EGL 20 hours post-BrdU were similar to those found in IGL approximately 20 days later (e.g., lobule I for all stages studied; VII and IX for day E16; II and X for day P1; VIb and X for day P5; IV, VIa, VIb, VIII for day P10 BrdU application; Fig. 11A–D). In lobule II, there was significant reduction in the number of future granule cells labeled at E16 when animals were allowed to survive until P20. That is, there were 50% fewer labeled cells determined in IGL at P20 than those found in EGL 20 hours post-BrdU (Fig. 11A). This evidence suggests that cells born in EGL may undergo apoptosis before entering the postmitotic zone, in agreement with studies in the rat EGL (Tanaka and Marunouchi, 1998), or labeled daughter cells may continue to proliferate, diluting label so that it is not detected (Hayes and Nowakowski 2002). These data clearly show that the survival index differed both across lobules and as a function of the stage examined, showing a need for further work on the systematic variation of cell cycle parameters and cell death events during lobule development.

To reveal any trend in the proliferation and survival pattern, we grouped the cerebellar lobules into archicerebellum (lobules I–VIa), neocerebellum (lobules VIb–VII), and paleocerebellum (lobules VIII–X; vestibulocerebellum: lobules X and ventral IX), based on the proposed anatomical, functional, and developmental criteria (Altman, 1969; Shiga et al., 1983; Lau et al., 1998; Podklet-

Fig. 7. Final position of labeled cells within the cerebellar internal granular layer after long-term survival. Photomicrographs of parasagittal sections of cerebellar cortex of lobule VII by day P20, following BrdU application at days P1 (**A**), P5 (**B**), and P10 (**C**). The vast majority of the labeled cells born at P1, P5 and P10 migrated away from the EGL by P20 and occupied the IGL. Asterisks indicate PC somata. IGL, internal granular layer; mol, molecular layer; PC, Purkinje cell somata. Scale bar = 20 μm.

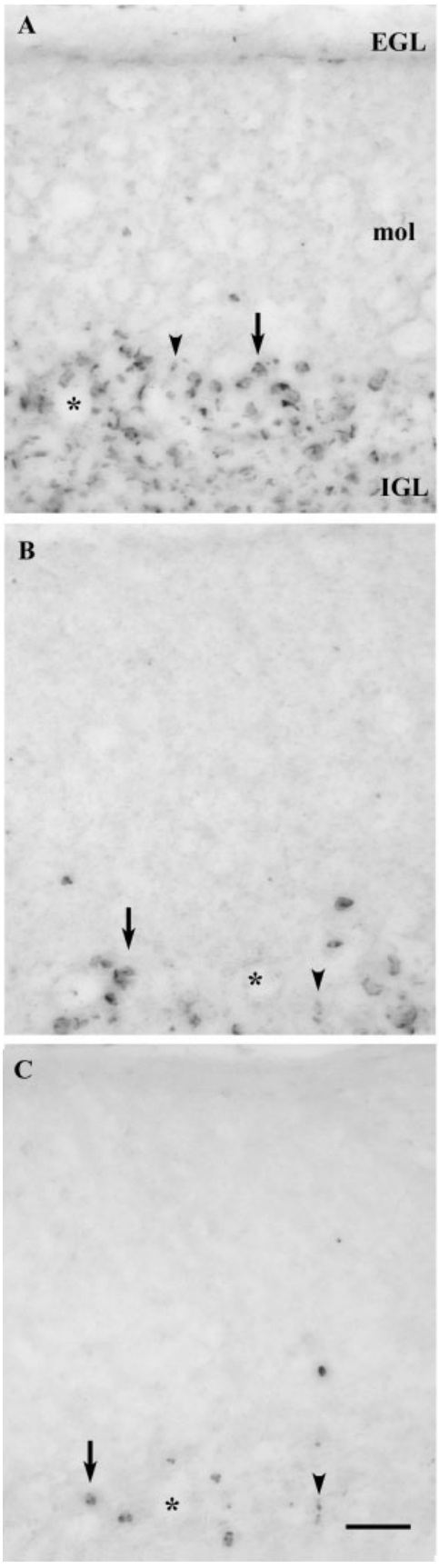

nova and Alho, 1998). This classification of lobular cell birth and survival according to phylogenetic categories showed that archicerebellum and paleocerebellum included the greatest increases in the final number of IGL labeled granule cells compared with their labeled EGL precursor population (Fig. 12A). In addition, by grouping the lobules into anterior (I–V) and posterior (VI–X) lobes (Fig. 12B) or ventral (I, II, III, VIII, IX, X) and dorsal (IV–VII) cerebellum (Fig. 12C), we found a significantly greater cell proliferation (number of cells labeled at 20 hours post-BrdU; Fig. 12B,C, open bars) and survival (number of labeled cells in IGL at long survival; Fig. 12B,C, solid bars) in the posterior lobe compared with the anterior, whereas dorsal cerebellar lobules showed relatively higher rates of cell production compared with ventral ones.

DISCUSSION

There is significant cell proliferation and neuron birth after hatching in the quail cerebellum, and, although cell proliferation is found in all of the cerebellar layers, the overwhelming majority is localized in the EGL. Cell birth continues through at least P50, although the rate after P20 is low. Protracted cell production in the cerebellum is not a species peculiarity; it has been observed in another precocial bird (young chicks; Dermon, unpublished observations). The vast majority of newborn neurons produced during the posthatching period are likely granule cells based on their appearance, site of birth, and final destination to IGL by P20. However, the late embryonic and early posthatching generation of at least some nongranule cells is likely, as evidenced by the presence of labeled cells in the molecular layer in the long-term survival groups. Transient dividing cells in the cerebellar white matter could be proliferating oligodendrocytes, astroglia, or neuronal precursors that would ultimately differentiate into molecular layer interneurons, as suggested for mammals (Zhang and Goldman, 1996).

The short survival experiments likely represent less than the cell cycle length plus the waiting in the deep EGL (Fujita et al., 1966; Rakic, 1971, 1973; Caviness et al., 1995; Komuro et al., 2001; Nowakowski et al., 2002). On the other hand, long survival experiments integrate proliferation, migration, and cell death events. It is established that the number of cells labeled by BrdU changes dramatically with time as a function of the number of proliferating cells in the population, length of S phase, length of the cell cycle, and cell death (Hayes and Nowakowski, 2002). Long survival data clearly showed that in most cases the total number of EGL labeled cells increased two- to fourfold compared with the proliferating population at 20 hours post-BrdU (Fig. 11). When EGL labeled

Fig. 8. Final position of labeled cells within the cerebellar layers after long-term survival. Photomicrographs of parasaggital sections of cerebellar cortex of lobule II by day P20, following BrdU application at E15 (**A**), E16 (**B**), and P1 (**C**). Most of the labeled cells born at E15, E16, and P1 migrated away from the EGL by P20 and occupied the granular cell layer. Note the presence of a population of labeled cells around PC, in addition to granule cells. Arrows indicate medium-sized and arrowheads small labeled cells close to PC. Asterisks indicate PC somata. EGL, external granular layer; IGL, internal granular layer; mol, molecular layer; PC, Purkinje cell somata. Scale bar = 20 μm.

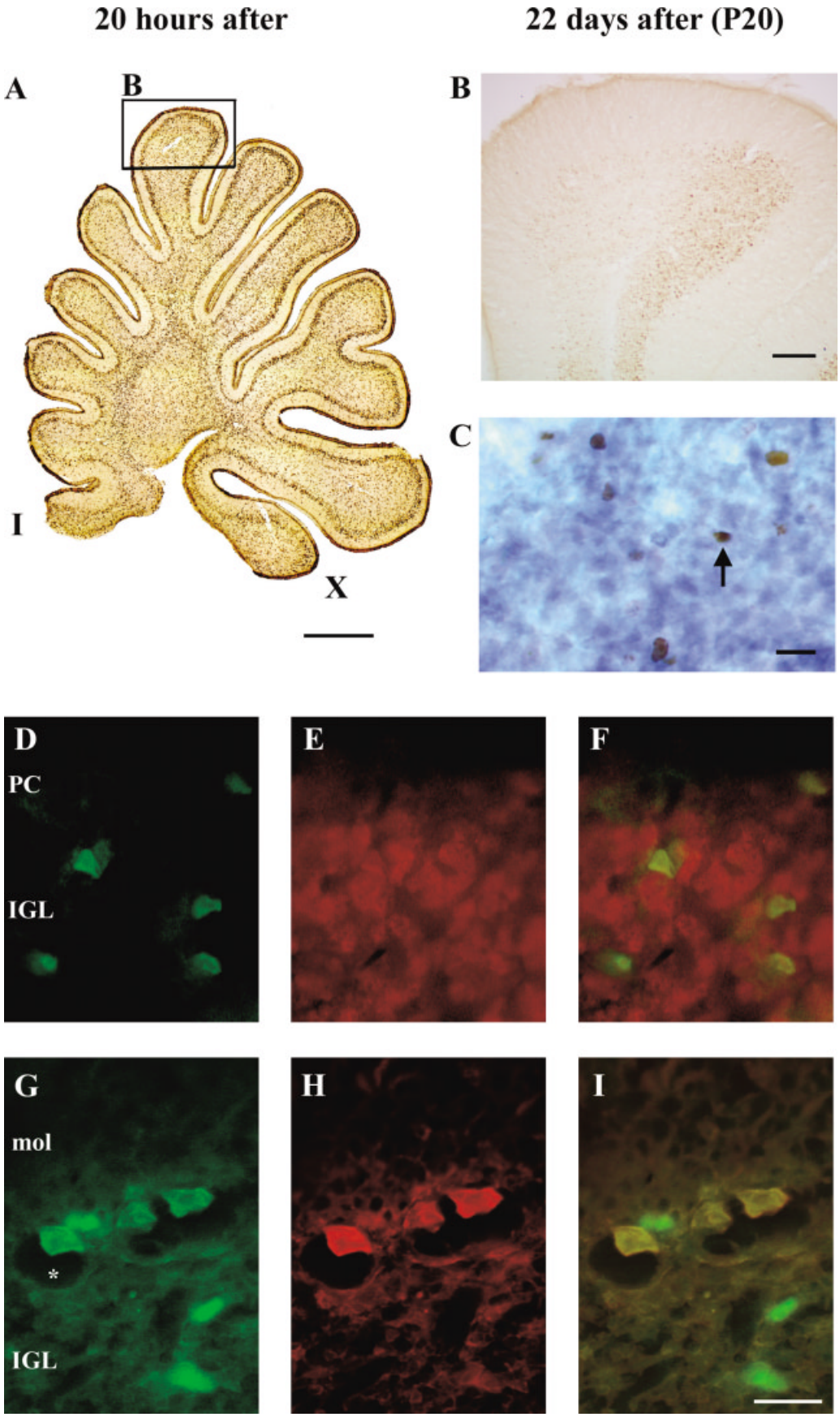

Figure 9

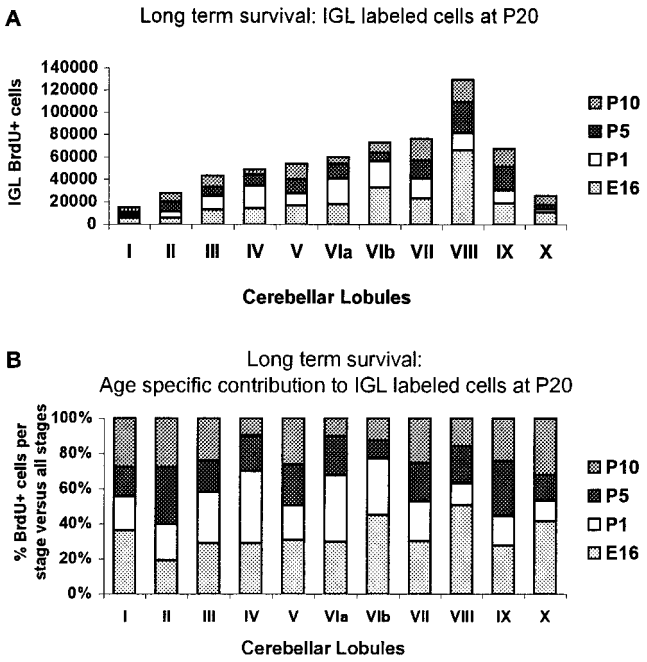

Fig. 10. Long survival experiments: age-specific EGL-labeled cells encountered in IGL at P20. **A:** The contribution of specific developmental stages to the total of labeling in the IGL is shown as stacks in the bars, with earlier stages at the bottom of the bars. **B:** Lobular pattern of the percentage of $BrdU^+$ cells labeled at a specific stage vs. the total $BrdU^+$ cells at all stages studied. The patterns indicating the ages are shown at right.

cells continue to divide, they may produce labeled proliferative cells (P), postmitotic labeled cells (Q cells), or both. If this process continues for three or more divisions, labeling is diluted and no longer detectable. For every labeled proliferating cell in EGL at specific developmental stage, there will be three or four labeled granule cells in IGL at P20 (if the third division is terminal and produces two postmitotic cells), based on the assumption that development is at steady state (i.e., P = Q = 0.5) and the hypothesis that P cells remain labeled for three (or more) cell cycles (Hayes and Nowakowski, 2002). This is a hypothetical maximal ratio assuming Q/P = 1 and not taking into account cell death. Our data showing a maximum of three to four times more labeled cells at P20 than at 20 hours post-BrdU in selected lobules at specific stages of the posterior cerebellar lobe suggest a prolonged development at posthatching stages. This pattern was noted specifically

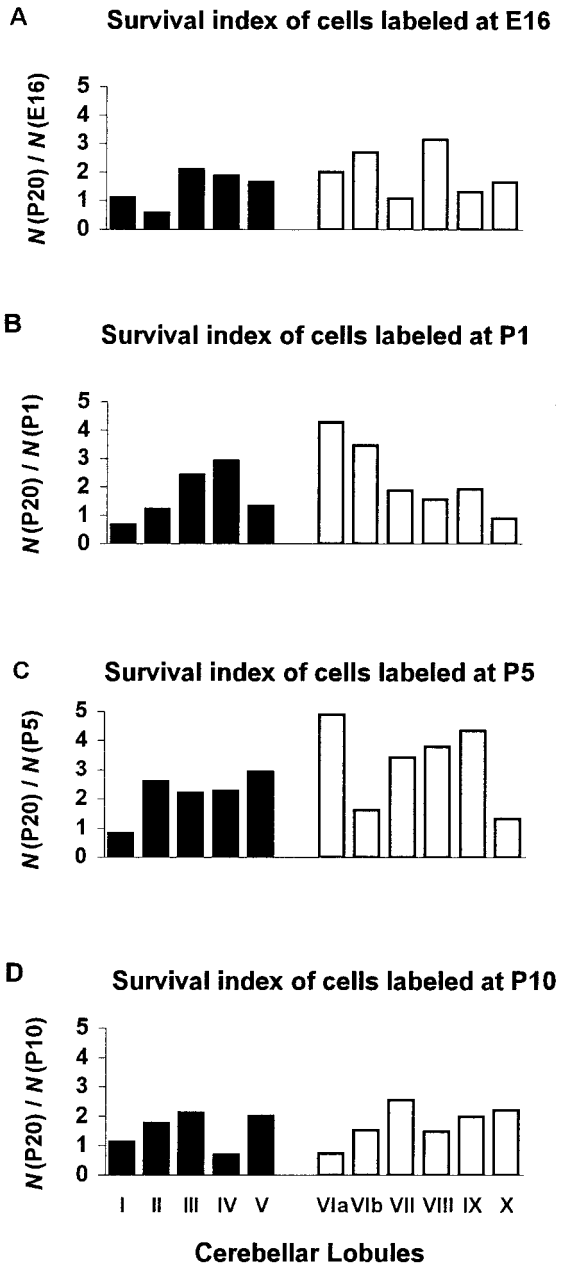

Fig. 11. Comparison of $BrdU^+$ cells labeled at the same stage at long and short survivals. Labeled cells encountered in the IGL at P20 vs. their progenitor cells in the EGL 20 hours post-BrdU. Survival is expressed as the ratio between the IGL positive cells by day P20 and the EGL labeled cells 20 hours post-BrdU administration at E16 (**A**), P1 (**B**), P5 (**C**), and P10 (**D**). Note that in most lobules there is a two- to fourfold increase in the number of labeled cells at long survival, suggesting their further division.

Fig. 9. Topography of proliferation and survival of granule cells and cell type characterized by double labeling. **A:** Photomicrograph of parasagittal section of the cerebellum, showing the distribution of labeled cells 20 hours post-BrdU application at day E15. Note that there is no rostrocaudal pattern within lobules in EGL labeling. **B:** Final position of E15 labeled cells, encountered after long survival at P20, in lobule VIa. A clear rostrocaudal topography is shown in the IGL labeling. **C:** Photomicrograph showing double labeling of NADPH-diaphorase and BrdU; arrow points to double-labeled cell ($BrdU^+$ expressing NOS); blus, diaphorase-positive cells; brown, $BrdU^+$ cells. **D–F:** Fluorescence photomicrographs showing double-labeled cells with BrdU and NeuN immunoreactivity. D: BrdU labeled, green; E: NeuN labeled, red; F: yellow double-labeled, single-labeled NeuN, red. **G–I:** Fluorescence photomicrographs showing double-labeled cells with BrdU and GAD immunoreactivity. G: $BrdU^+$, green; H: GAD^+, red; I: double-labeled, yellow; single $BrdU^+$, green. Anterior is leftward, dorsal is toward top. Asterisk indicates PC. IGL, internal granular layer; mol, molecular layer; PC, Purkinje cell soma. Scale bar in A = 500 μm; bar in B = 150 μm; bar in C = 20 μm; bar in I = 20 μm for D–I.

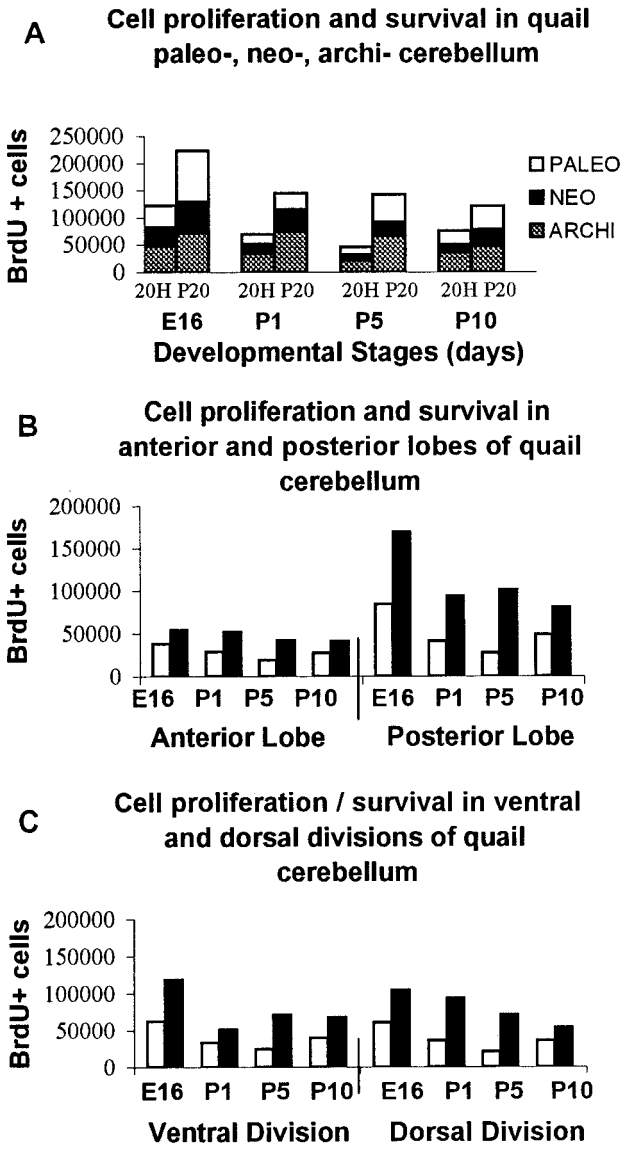

Fig. 12. Cell proliferation and survival in different cerebellar compartments grouped into phylogenetic categories. **A:** Anterior-posterior compartments. **B:** Dorsoventral divisions. **C:** Comparisons of the number of labeled cells at P20 and 20 hours post-BrdU injections at E16, P1, P5, and P10 in the paleo-, neo-, and archicerebellum (A), anterior (lobules I–V) and posterior lobe (lobules VIa–X; B), and ventral (I, II, III, VIII, IX, X) and dorsal (IV–VII) compartments (C) of the quail cerebellum. Open and solid bars in B and C show the number of labeled cells 20 hours post-BrdU and after long survival at day P20, respectively.

in lobule VIII at E16; in lobules VIa and VIb at P1; and in lobules VIa, VII, VIII, IX at P5. Our data thus suggest that, in most lobules, EGL labeled cells divide several times before exiting the cell cycle and migrate into the IGL. However, the factors affecting the observed labeling, including the Q/P ratio, and cell death likely differ for distinct cerebellar lobules and developmental stages.

Genesis of EGL cells at late stages

The most populous cell type in the cerebellum, the granule cells, derives from precursors in EGL, a displaced proliferative epithelium thought to produce exclusively granule neurons that settle in the granular layer within 0.5–3 days after their final division (Fujita et al., 1966; Altman, 1969; Hallonet et al., 1990; Alvarez Otero et al., 1993; Napieralski and Eisenman, 1993; Gao and Hatten, 1994; Alder et al., 1996; Jankovski et al., 1996; Zhang and Goldman, 1996). We suggest that most of the labeled cells in the posthatching quail cerebellum are granule cell precursors and that the locus of cell proliferation is the EGL. Preliminary experiments with shorter survival periods (3 or 6 hours) showed no apparent difference in the location of cell birth, although the density of newborn cells was lower than that after 20 hours of survival. These data support the idea that labeled cells consist of a population of granule cell precursors. Contrary to previous ideas that the avian EGL disappears at late embryonic stages or shortly after hatching (Hanaway, 1968), the quail EGL produces new cells even at posthatching day 50, although at a progressively declining rate. Ramon y Cajal (1911) distinguished a superficial site of the EGL, the germinal zone, and a deeper zone of differentiating granule cells, the premigratory zone (Altman et al., 1968; Altman, 1972). Similarly, it is well established that, at earlier stages, avian EGL cells proliferate in the superficial layer and give rise to postmitotic cells that migrate tangentially within the deeper layers of the EGL (Hallonet et al., 1990; Ryder and Cepko, 1994). It has been suggested that mammalian postmitotic granule cells can remain in the EGL for at least 20 hours (Rakic, 1971; Komuro et al., 2001) before moving to the IGL. In agreement with this, the present data suggest that, after their last division, avian granule cells remain in the EGL for from a few hours to many days; we saw labeled cells in the EGL 10–20 days post-BrdU injection. The labeled EGL cells were capable of migrating through the molecular layer, as suggested by their elongated appearance, typical of migrating granule cells, and a few were found in the molecular layer, in close association with glial fibrillary acidic protein (GFAP)-positive radial glial fibers (data not shown). However, we did not identify parasagittal streams of cells described as "granule cell raphes" (Lin and Cepko, 1998; Karam et al., 2000), because of the late stages studied. Such a nonribboned migration is thought by Komuro and Rakic (1998) to occur in late developmental stages in mammals. However, we did identify the topographic distribution of labeled cells in EGL areas of dense labeling, noted mostly at the tips of the lobules and interrupted by quiet regions. Long-term survival (approximately 20 days) post-BrdU application resulted in the addition of most labeled cells to the IGL, suggesting that the EGL labeled cells had reached their final destination. Moreover, they survived at least until day P50, suggesting their normal integration into the cerebellar circuitry.

Genesis of other cell populations

Different cell types in the cerebellum have distinct ontogenetic periods as well as specific sites of precursor proliferation in the EGL and ventricular neuroepithelium. Our short survival data show that molecular interneurons are born during the late embryonic stages (E15, E16), in agreement with previous studies, although we did not define their site of birth. It is not clear whether they originate in the ventricular or EGL germinal zone. Mammalian basket and stellate cells are born at a time when no mitotic activity is observed in the ventricular layer

(Miale and Sidman, 1961). Therefore, it has been proposed that their neuronal progenitors arise from the ventricular zone, migrate toward the molecular layer, and continue to divide in the cerebellar white matter, until settling in their final position (Zhang and Goldman, 1996). Studies employing birth dating with ^{3}H-thymidine and quail-chick chimeras also suggest that molecular layer interneurons are likely produced by progenitors dividing in the ventricular epithelium and not in the EGL (Hanaway, 1968; Yurkewicz et al., 1981; Kanemitsu and Kobayashi, 1988; Hallonet et al., 1990; Hallonet and Le Douarin, 1992; Alvarez Otero et al., 1993; Napieralski and Eisenman, 1993). In contrast, it has been suggested that Golgi neurons (Hausmann et al., 1985), cells of the isthmus and rostral hindbrain (Lin et al., 2001), derive from EGL. In the present study, there was significant labeling in the white matter 20 hours post-BrdU injection at E15, coinciding with the appearance of a cell population in the molecular layer found around PC. After long survival (at P20), when cells labeled at E15 were no longer present in the white matter, a BrdU$^+$ cell population about 10 μm in diameter, doubly labeled with GAD, was located around PC. This evidence suggests that cells proliferating at E15 and settling at P20 around PC may be basket interneurons, based on their final location and GAD immunoreactivity. We could not identify any trend of cells from the white matter migrating toward the molecular layer but cannot exclude the possibility that these cells became postmitotic within the white matter, as has been suggested for the mammalian molecular layer interneurons. However, insofar as the more active proliferating zone at these stages is EGL, it is also possible that at least part of these cell populations is derived from the EGL. Consistent with this idea is our observation that generation of cell types residing in the molecular layer continued at a lower rate in most lobules until P10, although, at posthatching days P1–P10, we could see only a few labeled cells in the white matter.

In addition, it is known that glia develop at late stages (Shiga et al., 1983; Reynolds and Wilkin, 1991). Glioblasts are thought to originate from the ventricular epithelium and to divide in situ, but their exact course of development in the avian cerebellum is not known (Hanaway, 1968; Altman, 1969). In the present study, we did detect small BrdU$^+$ cells in the Purkinje cell layer, 2–3 μm in diameter. It has been suggested that small cells surrounding Purkinje cell bodies in chick cerebellum are formed by glia cell precursors dividing in the IGL (Hanaway, 1968), even though the glial nature of these cells has not yet been confirmed (Hallonet and Mallart, 1997). In addition, it is known that some cells continue to proliferate within the IGL, although their final position and phenotype remain unclear (Fujita et al., 1966). Of great importance in this context are recent studies providing evidence for the generation of neurons from glial precursors (e.g., Malatesta et al., 2000; Seri et al., 2000; Noctor et al., 2001; Parnavelas and Nadarajah, 2001). Whether a population of the labeled cells in the quail cerebellum could also be characterized as multipotent progenitors that can generate both neurons and glia remains to be established.

Functional implications

The observed trend for late proliferation of granule cell precursors in quail cerebellum followed, in part, the previously suggested pattern for the rat, that is, ventral to dorsal maturation, with the phylogenetically younger neocerebellum ending its ontogenesis last (Altman, 1969). In addition, our data suggest that, at late developmental stages, a greater proportion of granule cells were born and survived in the caudal cerebellar cortex. This pattern of late granule cells genesis relates well with the pattern of later Purkinje cell generation in the posterior chick cerebellum (Yurkewicz et al., 1981), in the context of the modular cerebellar organization in parasagittal territories (Karam et al., 2001; Blanco et al., 2002). In addition, the different origins of anterior and posterior cerebellum, as shown from chick-quail chimeric embryos, could account for this difference in proliferation pattern. That is, part of the rostral cerebellum originates from the so-called mesencephalic alar plate (Martinez and Alvarado-Mallart, 1989), whereas caudal cerebellum originates from the metencephalic alar plate (Hallonet et al., 1990). Moreover, the division into anterior and posterior domains is supported by the complementary pattern of different Eph receptors and ephrins (Karam et al., 2000; Blance et al., 2002).

The cerebellum is considered a major brain center for motor control, sensory association (Herrup and Kuemerle, 1997), and high-order cognitive functions, such as learning and memory (Thach, 1998; Hikosaka et al., 1998; Middleton and Strick, 2000). Our quantitative results suggest that granule cells born after hatching survive into adulthood and become incorporated into the cerebellar network. In the same early posthatch period, extensive expansion of dendritic arborization of PC occurs in quail cerebellum, and the formation of parallel fiber synapses on distal dendrites has been suggested (Mori and Matsushima, 2002). The period of rapid dendritic growth and active synaptogenesis coincides with the observed late granule cell genesis, supporting the hypothesis of their incorporation into the cerebellar circuits. It has been shown that, in meander tail mouse cerebellum, multipotent progenitors derived from the EGL could differentiate into neurons and compensate for granule cell death (Rosario et al., 1997). This evidence suggests a developmental mechanism with many implications, including motor learning plasticity. In archicerebellar lobules III and IV, neurons were born in the EGL at a rate that deviated very little with age, suggesting a prolonged maturation period and a possible extended developmental window for plastic responses to internal or external changes. In the pigeon, there is a somatotopic representation of the wings in lobules III–V (Necker, 2001). If the same representation exists in the quail cerebellum, the newborn cells could be integrated in circuits for motor control of the wings. At the behavioral level, cell birth in lobules III–V may be correlated with cerebellar participation in motor control, in that, during this posthatching period, the quails start jumping and making their first flight attempts. It would be most interesting to test whether interference with neurogenesis at this time would affect the training and execution of such motor programs. Moreover, interference with the motor behavior of the animal could affect proliferation, migration, or survival. If substantiated through further study, this would provide another example of the role of neurogenesis in modifying a motor circuit, as has been shown for song learning in canaries (Goldman and Nottebohm, 1983; Alvarez-Buylla et al., 1990a,b; Kirn and Nottebohm, 1993).

ACKNOWLEDGMENTS

The authors thank Prof. R. Nowakowski for most useful comments on the manuscript. We thank graduate students B. Zikopoulos, C. Ambatzis, and L. Panagis for excellent technical assistance for the revised form of the article.

LITERATURE CITED

Alder J, Cho NK, Hatten ME. 1996. Embryonic precursor cells from the rhombic lip are specified to a cerebellar granule neuron identity. Neuron 17:389–399.

Altman J. 1969. Autoradiographic and histological studies of postnatal neurogenesis. III. Dating the time of production and onset of differentiation of cerebellar microneurons in rats. J Comp Neurol 136:269–294.

Altman J. 1972. Postnatal development of the cerebellar cortex in the rat. I. The external germinal layer and the transitional molecular layer. J Comp Neurol 145:353–398.

Altman J, Anderson WJ, Wright KA. 1968. Differential radiosensitivity of stationary and migratory primitive cells in the brains of infant rats. Exp Neurol 22:52–74.

Alvarez-Buylla A, Kirn JR, Nottebohm F. 1990a. Birth of projection neurons in adult avian brain may be related to perceptual or motor learning. Science 249:1444–1446.

Alvarez-Buylla A, Theelen M, Nottebohm F. 1990b. Proliferation "hot spots" in adult avian ventricular zone reveal radial cell division. Neuron 5:101–109.

Alvarez Otero R, Sotelo C, Alvarado-Mallart RM. 1993. Chick-quail chimeras with partial cerebellar grafts: an analysis of the origin and migration of cerebellar cells. J Comp Neurol 333:597–615.

Bannigan J, Langman J. 1979. The cellular effect of 5-bromodeoxyuridine on the mammalian embryo. J Embryol Exp Morphol 50:123–135.

Benagiano V, Virgintino D, Rizzi A, Flace P, Troccoli V, Bormann J, Monaghan P, Robertson D, Roncali L, Ambrosi G. 2000. Glutamic acid decarboxylase-positive neuronal cell bodies and terminals in the human cerebellar cortex. Histochem J 32:557–564.

Blanco MJ, Pena-Melian A, Nieto MA. 2002. Expression of EphA receptors and ligands during chick cerebellar development. Mech Dev 114:225–229.

Cavalieri B. 1966 [reprint]. Geometria degli indivisibili. Torino: Unione Tipografico-Editrice Torinese.

Caviness VS, Takahashi T, Nowakowski RS. 1995. Numbers, time and neocortical neuro-genesis: a general developmental and evolutionary model. Trends Neurosci 18:379–383.

De Zeeuw CI, Wylie DR, DiGiorgi PL, Simpson JI. 1994. Projections of individual Purkinje cells of identified zones in the flocculus to the vestibular and cerebellar nuclei in the rabbit. J Comp Neurol 349:428–448.

Dermon CR, Stamatakis A. 1994. Laminar pattern of NADPH-diaphorase activity in the developing avian cerebellum. Neuroreport 5:1941–1945.

Dermon CR, Zikopoulos B, Panagis L, Harrison E, Lancashire CL, Mileusnic R, Stewart MG. 2002. Passive avoidance training enhances neuron proliferation in day old chicks. Eur J Neurosci 16:1267–1274.

Dombrowski S, Barbas H. 1996. Differential expression of NADPH diaphorase in functionally distinct prefrontal cortices in the rhesus monkey. Neuroscience 72:49–62.

Feirabend HK. 1990. Development of longitudinal patterns in the cerebellum of the chicken (*Gallus domesticus*): a cytoarchitectural study of the genesis of cerebellar modules. Eur J Morphol 28:169–223.

Fujita S. 1962. Kinetics of cellular proliferation. Exp Cell Res 28:52–60.

Fujita S, Shimada M, Nakamura T. 1966. *3*H-thymidine autoradiographic studies on the cell proliferation and differentiation in the external and the internal granular layers of the mouse cerebellum. J Comp Neurol 128:191–208.

Gao W-Q, Hatten ME. 1994. Immortalizing oncogenes subvert the establishment of granule cell identity in developing cerebellum. Development 120:1059–1070.

Goldman SA, Nottebohm F. 1983. Neuronal production, migration, and differentiation in a vocal control nucleus of the adult female canary brain. Proc Natl Acad Sci U S A 80:2390–2394.

Gundersen HJ, Bagger P, Bendtsen TF, Evans SM, Korbo L, Marcussen N, Moller A, Nielsen K, Nyengaard JR, Pakkenberg B, Serensen FB, Vesterby A, West MJ. 1988. The new stereological tools: disector, fractionator, nucleator and point sampled intercepts and their use in pathological research and diagnosis. Acta Pathol Microbiol Immunol Scand 96:857–881.

Hallonet M, Alvarado-Mallart RM. 1997. The chick/quail chimeric system: a model for early cerebellar development. Perspect Dev Neurobiol 5:17–31.

Hallonet ME, Le Douarin NM. 1993. Tracing neuroepithelial cells of the mesencephalic and metencephalic alar plates during cerebellar ontogeny in quail-chick chimaeras. Eur J Neurosci 5:1145–1155.

Hallonet ME, Teillet M-A, Le Douarin NM. 1990. A new approach to the development of the cerebellum provided by the quail-chick marker system. Development 108:19–31.

Hanaway J. 1967. Formation and differentiation of the external granular layer of the chick cerebellum. J Comp Neurol 131:1–14.

Hanaway J. 1968. Origin of basket cells in the molecular layer of the chick cerebellum. Anat Rec 160:360.

Hausmann B, Mangold U, Sievers J, Berry M. 1985. Derivation of cerebellar Golgi neurons from external granular layer: evidence from explantation of external granule cells in vivo. J Comp Neurol 232:511–522.

Hayes NL, Nowakowski RS. 2000. Exploiting the dynamics of S-phase tracers in developing brain: interkinetic nuclear migration for cells entering vs. leaving the S-phase. Dev Neurosci 22:44–45.

Herrup K, Kuemerle B. 1997. The compartmentalization we are keenly aware. Annu Rev Neurosci 20:61–90.

Hikosaka O, Miyashita K, Miyachi S, Sakai K, Lu X. 1998. Differential roles of the frontal cortex, basal ganglia, and cerebellum in visuomotor sequence learning. Neurobiol Learn Mem 70:137–149.

Ito M. 2000. Mechanisms of motor learning in the cerebellum. Brain Res 886:237–245.

Ito M, Orlov I, Yamamoto M. 1982. Topographical representation of vestibulo-ocular reflexes in rabbit cerebellar flocculus. Neuroscience 7:1657–1664.

Jankovski A, Rossi F, Sotelo C. 1996. Neuronal precursors in the postnatal mouse cerebellum are fully committed cells: evidence from heterochronic transplantations. Eur J Neurosci 8:2308–2319.

Kanemitsu A, Kobayashi Y. 1988. Time of origin of Purkinje cells and neurons of the deep cerebellar nuclei of the chick embryo examined by ^{3}H-thymidine autoradiography. Anat Anz 165:167–175.

Karam SD, Burrows RC, Logan C, Koblar S, Pasquale EB, Bothwell M. 2000. Eph receptors and ephrins in the developing chick cerebellum: relationship to sagittal patterning and granule cell migration. J Neurosci 20:6488–6500.

Karam SD, Kim YS, Bothwell M. 2001. Granule cells migrate within raphes in the developing cerebellum: an evolutionary conserved morphogenetic event. J Comp Neurol 440:127–135.

Kirn JR, Nottebohm F. 1993. Direct evidence for loss and replacement of projection neurons in adult canary brain. J Neurosci 13:1654–1663.

Kirn JR, Alvarez-Buylla A, Nottebohm F. 1991. Production and survival of projection neurons in a forebrain vocal center of adult male canaries. J Neurosci 11:1756–1762.

Komuro H, Yacubova E, Yacubova E, Rakic P. 2001. Mode and tempo of tangential cell migration in the cerebellar external granular layer. J Neurosci 21:527–540.

Lau KL, Glover RG, Linkenhoker B, Wylie DR. 1998. Topographical organization of inferior olive cells projecting to translation and rotation zone in the vestibulocerebellum of pigeon. Neuroscience 85:605–614.

Le Douarin NM. 1993. Embryonic neural chimeras in the study of brain development. Trends Neurosci 16:64–72.

Lin JC, Cepko CL. 1998. Granule cell raphes and parasagittal domains of Purkinje cells: complementary patterns in the developing chick cerebellum. J Neurosci 18:9342–9353.

Lin JC, Cai L, Cepko CL. 2001. The external granule layer of the developing chick cerebellum generates granule cells and cells of the isthmus and rostral hindbrain. J Neurosci 21:159–168.

Malatesta P, Hartfuss E, Gotz M. 2000. Isolation of radial glial cells by fluorescent-activated cell sorting reveals a neuronal lineage. Development 127:5253–5263.

Marin F, Puelles L. 1995. Morphological fate of rhombomeres in quail/chick chimeras: a segmental analysis of hindbrain nuclei. Eur J Neurosci 7:1714–1738.

Martinez S, Alvarado-Mallard RM. 1989. Rostral cerebellum originates from the caudal portion of the so-called 'mesencephalic' vescicle: a study using chick/quail chimeras. Eur J Neurosci 1:549–560.

Miale IL, Sidman RL. 1961. An autoradiographic analysis of histogenesis in the mouse cerebellum. J Exp Neurol 4:277–296.

Middleton FA, Strick PL. 2000. Basal ganglia and cerebellar loops: motor and cognitive circuits. Brain Res Brain Res Rev 31:236–250.

Miller M, Nowakowski RS. 1988. Use of bromodeoxyuridine-immunohistochemistry to examine the proliferation, migration and time of origin of cells in the central nervous system. Brain Res 457:44–52.

Mori M, Matsushima T. 2002. Post-hatch development of dentritic arborization in cerebellar Purkinje neurons of quail chicks: a morphometric study. Neurosci Lett 329:73–76.

Mullen RJ, Buck CR, Smith AM. 1992. NeuN, a neuronal specific nucleuar protein in vertebrates. Development 116:201–211.

Napieralski JA, Eisenman LM. 1993. Developmental analysis of the external granular layer in the *Meanter Tail* mutant mouse: do cerebellar microneurons have independent progenitors? Dev Dyn 197:244–254.

Necker R. 2001. Spinocerebellar projections in the pigeon with special reference to the neck region of the body. J Comp Neurol 429:403–418.

Noctor SC, Flint AC, Weissman TA, Dammerman RS, Kriegstein AR. 2001. Neurons derived from radial glial cells establish radial units in neocortex. Nature 409:714–720.

Nowakowski RS, Caviness VS Jr, Takahashi T, Hayes NL. 2002. Population dynamics during cell proliferation and neuronogenesis in the developing murine neocortex. Results Probl Cell Differ 39:1–25.

Palay SL, Chan-Palay V. 1974. The cerebellar cortex. New York: Springer-Verlag.

Parnavelas JG, Nadarajah B. 2001. Radial glial cells: are they glia? Neuron 31:881–884.

Podkletnova I, Alho H. 1998. Neonatal noradrenaline depletion prevents the transition of Bergmann glia in the developing cerebellum. J Chem Neuroanat 14:167–173.

Rakic P. 1971. Neuro-glia relationship during granule cell migration in developing cerebellar cortex. J Comp Neurol 141:283–312.

Rakic P. 1973. Kinetics of proliferation and latency between final cell division and onset of differentiation of cerebellar stellate and basket neurons. J Comp Neurol 147:523–546.

Ramon y Cajal S. 1911. Histologie du systeme nerveux de l'homme et des vertebras. Paris: A. Maloine.

Reynolds R, Wilkin GP. 1991. Oligodendroglial progenitor cells but not oligodendroglia divide during normal development of the rat cerebellum. J Neurocytol 20:216–224.

Rosario CM, Yandava BD, Kosaras B, Zurakowski D, Sidman RL, Snyder EY. 1997. Differentiation of engrafted multipotent neural progenitors toward replacement of missing granule cell neurons in meander tail cerebellum may help determine the locus of mutant gene action. Development 124:4213–4224.

Ryder EF, Cepko CL. 1994. Migration patterns of clonally related granule cells and their progenitors in the developing chick cerebellum. Neuron 12:1011–1029.

Schultze B, Korr H. 1981. Cell kinetic studies of different cell types in the developing and adult brain of the rat and the mouse: a review. Cell Tissue Kinet 14:309–325.

Seri B, Garcia-Verdugo JM, McEwen BS, Alvarez-Buylla A. 2001. Astrocytes give rise to new neurons in the adult mammalian hippocampus. J Neurosci 21:7153–7160.

Shiga T, Ichikawa M, Hirata Y. 1983. Spatial and temporal pattern of postnatal proliferation of Bergmann glia cells in rat cerebellum: an autoradiographic study. Anat Embryol 167:203–211.

Spiro JE, Dalva MB, Mooney RJ. 1999. Long-range inhibition within the zebra finch song nucleus RA can coordinate the firing of multiple projection neurons. Neurophysiology 81:3007–3020.

Sterio DC. 1984. The unbiased estimation of number and sizes of arbitrary particles using the disector. J Microsc 134:127–136.

Striedter GF, Keefer BP. 2000. Cell migration and aggregation in the developing telencephalon: pulse-labeling chick embryos with bromodeoxyuridine. J Neurosci 20:8021–8030.

Tanaka M, Marunouchi T. 1998. Immunohistochemical analysis of developmental stage of external granular layer neurons which undergo apoptosis in postnatal rat cerebellum. Neurosci Lett 242:85–88.

Thach WT. 1998. A role for the cerebellum in learning movement coordination. Neurobiol Learn Mem 70:177–188.

Wassef M, Joyner AL. 1997. Early mesencephalon/metencephalon patterning and development of the cerebellum. Perspect Dev Neurobiol 5:3–16.

Wilson DB. 1973. Chronological changes in the cell cycle of chick neuroepithelial cells. J Embryol Exp Morphol 29:745–751.

Yu WHA. 1977. The effect of 5-bromodeoxyuridine on the postnatal development of the rat cerebellum: morphologic and radioautographic studies. Am J Anat 150:89–108.

Yurkewicz L, Lauder JM, Marchi M, Giacobini E. 1981. ^{3}H-thymidine long survival autoradiography as a method for dating the time of neuronal origin in the chick embryo: the locus coeruleus and cerebellar Purkinje cells. J Comp Neurol 203:257–267.

Zhang L, Goldman JE. 1996. Generation of cerebellar interneurons from dividing progenitors in white matter. Neuron 16:47–54.

Zikopoulos B, Kentouri M, Dermon CR. 2001. Cell genesis in the hypothalamus is associated to the sexual phase of a hermaphrodite teleost. Neuroreport 12:2477–2481.

Zupanc GKH, Horscke I. 1995. Proliferation zones in the brain of adult Gymnotiform fish: a quantitative mapping study. J Comp Neurol 353: 213–233.